

# Rethinking Token-Level Policy Optimization for Multimodal Chain-of-Thought

Yunheng Li<sup>\*1</sup>, Hangyi Kuang<sup>\*1</sup>, Hengrui Zhang<sup>1</sup>, Jiangxia Cao<sup>2</sup>, Zhaojie Liu<sup>2</sup>,  
Qibin Hou<sup>†1</sup>, Ming-Ming Cheng<sup>1</sup>

<sup>1</sup>VCIP, School of Computer Science, Nankai University

<sup>2</sup>Kuaishou Technology

<sup>\*</sup>Equal Contribution. <sup>†</sup>Corresponding author.

**Abstract:** Multimodal Chain-of-Thought (CoT) reasoning requires large vision-language models to construct reasoning trajectories that interleave perceptual grounding with multi-step inference. However, existing Reinforcement Learning with Verifiable Rewards (RLVR) methods typically optimize reasoning at a coarse granularity, treating CoT uniformly without distinguishing their varying degrees of visual grounding. In this work, we conduct a token-level analysis of multimodal reasoning trajectories and show that successful reasoning is characterized by structured token dynamics reflecting both perceptual grounding and exploratory inference. Building upon this analysis, we propose **Perception-Exploration Policy Optimization (PEPO)**, which derives a perception prior from hidden state similarity and integrates it with token entropy through a smooth gating mechanism to produce token-level advantages. PEPO integrates seamlessly with existing RLVR frameworks such as GRPO and DAPO, requiring neither additional supervision nor auxiliary branches. Extensive experiments across diverse multimodal benchmarks demonstrate consistent and robust improvements over strong RL baselines, spanning geometry reasoning, visual grounding, visual puzzle solving, and few-shot classification, while maintaining stable training dynamics.

**Project Page:** <https://github.com/xzxxntxdy/PEPO>

HVision@Nankai

## 1 Introduction

Large Vision-Language Models (LVLMs) [3, 88, 64, 21, 58, 75] have achieved impressive progress across diverse vision-language tasks, such as question answering [2, 18], visual reasoning [36, 83, 45, 46] and reasoning grounding [25, 78, 27]. Recent advances in LVLMs [51, 71, 38, 33, 32, 7, 66, 89, 80] have focused on enhancing their reasoning capability, where Reinforcement Learning (RL) serves as an effective way to optimize Chain-of-Thought (CoT) [68] reasoning and improve performance.

Typical LVLM training pipelines incorporate RL with verifiable rewards to refine CoT reasoning, commonly under frameworks such as Group Relative Policy Optimization (GRPO) [19, 50]. For example, most approaches adopt outcome-based rewards (e.g., format or accuracy) under the assumption that improving answer format or textual correctness naturally leads to coherent reasoning. However, these methods suffer from sequence-level supervision, which fails to distinguish the contributions of intermediate CoT steps. To mitigate this, several works in Large Language Models (LLMs) introduce token-level entropy advantages to encourage exploration at uncertain CoT steps [62, 8, 63]. Nevertheless, entropy-based advantages mainly capture textual uncertainty but show weak correspondence to visual semantics and insufficient discrimination of reasoning relevance. Recent perception-aware RL methods incorporate visual signals, but often introduce additional computational overhead through auxiliary masking branches [67, 20] or attention-based measures [22] that are incompatible with efficient acceleration frameworks [13].

Unlike text-only LLMs, LVLMs reason under multimodal constraints, where visual perception and exploratory dynamics play complementary roles in shaping the CoT process, as illustrated in Fig. 1(a). From the perceptual perspective, token-level analysis in Sec. 3.2 reveals that correct reasoning is strongly associated with perceptual grounding: accurate responses consistently depend on a compact subset of visually aligned tokens that anchor the CoT process. More importantly, a simple hidden-state similarity between response and visual tokens captures

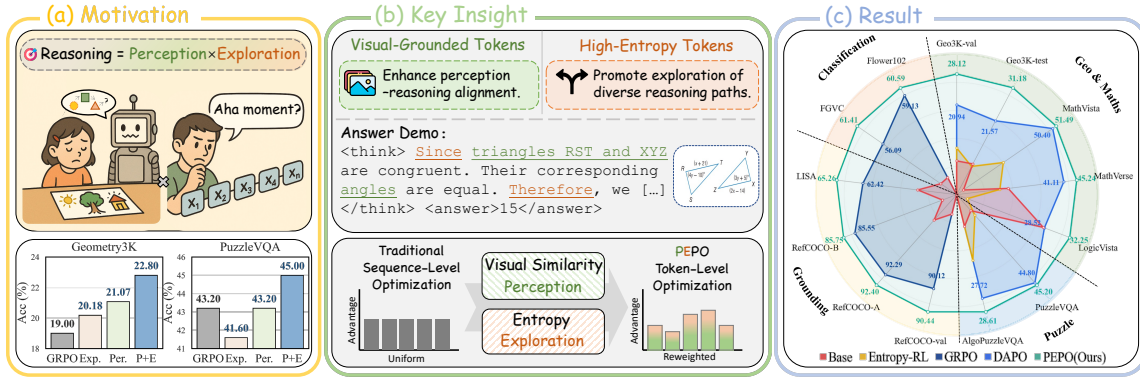


**Figure 1** Overview of PEPO. (a) Effective multimodal reasoning arises from the complementarity between perception and exploration. Abbr. Exp.: Exploration-only, Per.: Perception-only, P+E: Perception + Exploration. (b) Unlike traditional sequence-level optimization with uniform advantages, PEPO reweights tokens using a perception prior from visual similarity and entropy via a smooth gate, producing fine-grained token-level advantages. (c) When integrated with GRPO or DAPO, PEPO consistently improves performance across diverse benchmarks.

this association, providing a modality-specific indicator within the fine-grained reasoning process and reflecting linguistic-perceptual alignment. Complementing perception, token-level entropy from the logits highlights uncertain steps where alternative reasoning paths should be explored. However, we find that existing RLVR frameworks overlook the fine-grained coupling between perceptual grounding and reasoning dynamics, relying mainly on outcome- or entropy-based supervision, as well as mask-based perception-aware methods that fail to capture modality-specific interactions.

Motivated by the aforementioned analysis, we introduce Perception-Exploration Policy Optimization (PEPO), a token-level policy optimization framework that couples visual perception and exploration to enhance CoT reasoning in LVLMs. The core of PEPO is to convert hidden-state similarity into a calibrated perception prior without auxiliary branches or additional supervision. Specifically, for each response token, we compute cosine similarity between its hidden state and the set of visual-token states and aggregate it into a per-token visual grounding score. To incorporate exploration in a unified manner, PEPO employs a smooth gating mechanism that fuses token-level entropy from the logits with the perception prior to produce a normalized token weight. These weights refine the sequence-level advantage into token-level advantages, thereby reweighting the policy-gradient updates toward visual-grounded and exploratory reasoning tokens. Moreover, PEPO integrates seamlessly with GRPO (PEPO<sub>G</sub>) and DAPO [79] (PEPO<sub>D</sub>), providing fine-grained optimization signals with only marginal computational overhead.

To validate the effectiveness of PEPO, we evaluate it across multiple multimodal reasoning benchmarks, including geometry and math/logic reasoning, visual puzzles, visual grounding, and few-shot classification. Across Geometry3K [37], MathVista-mini [36], MathVerse-mini [83], and LogicVista [72], PEPO improves over GRPO [19, 50] by +3.67 points on Qwen2.5-VL-3B [3] and by +3.51 points on InternVL3-2B [88], and over DAPO [79] by +0.45 and +5.15 points, respectively. On visual puzzles (PuzzleVQA and AlgoPuzzleVQA [10]), PEPO yields gains of +1.65 and +1.52. For visual grounding (RefCOCO [78] and LISA-Grounding [27]), PEPO achieves +0.86 IoU@50 improvement while avoiding the entropy-only collapse. In few-shot classification (FGVC Aircraft [39] and Flower102 [43]), it improves accuracy by +5.32 and +1.46. Furthermore, scalability analysis on ViRL39k [61] shows that perception-exploration coupling consistent gains with larger data scales, indicating robust generalization and optimization stability across multimodal tasks. To sum up, our main contributions are threefold:

- To our knowledge, this is the first work to explore the complementary roles of visual-grounded and high-entropy tokens in LVLMs, revealing how perception anchors reasoning while entropy drives exploration.
- We propose PEPO, a token level policy optimization framework that derives a perception prior from hidden state similarity and incorporates entropy through a smooth gating mechanism to refine advantage estimation.
- We instantiate PEPO<sub>G</sub> and PEPO<sub>D</sub> on GRPO and DAPO and obtain consistent gains across geometry, math

and logic, visual puzzles, visual grounding, and few-shot classification with marginal overhead.

## 2 Related Work

**RLVR for LVLMs.** Reinforcement learning with verifiable rewards [9, 50, 19, 79] has become an effective approach for training LVLMs. Among RLVR methods, GRPO is widely used for its stable and critic-free design that directly leverages verifiable rewards for policy optimization. Recent research has advanced this framework along two main lines of work. Data-centric studies construct large-scale multimodal datasets and adaptive training schedules to improve generalization [76, 31, 40, 46, 65, 1, 6, 81, 4, 64, 14]. Meanwhile, reward-centric methods design verifiable rewards for multimodal tasks, such as visual grounding and question answering [52, 34, 17, 77, 24, 42, 53, 23, 29, 28, 70]. Despite these advances, they still rely on sequence-level supervision that overlooks token-level perceptual and reasoning differences. Recent efforts have explored token-level refinement via entropy-based optimization [62, 8, 63, 11, 59], but these methods primarily focus on stabilizing policy updates or enhancing exploration in text-only domains, resulting in limited improvements in LVLm training.

**Reasoning in LVLMs.** Reasoning has emerged as a key capability for advancing LVLMs, enabling multi-step inference, numerical computation, and structured visual understanding [55, 5, 44]. Existing approaches enhance reasoning in LVLMs through chain-of-thought supervision and step-wise instruction tuning [73, 84, 41], which encourage structured inference but remain limited by static supervision and lack adaptive feedback. To address this, reinforcement learning has been employed to refine reasoning consistency and correctness [61, 60, 15, 9], introducing dynamic optimization signals for reasoning refinement. Recent RL-based studies further incorporate verifiable or task-specific rewards for logical reasoning, mathematical derivation, and spatial problem solving [57, 29, 51, 71, 38, 33]. Meanwhile, an emerging line of work operationalizes perception as tool use, employing visual operations such as cropping and zooming [69, 85, 48, 74, 54, 87, 16, 90]. Nevertheless, existing RL-based reasoning frameworks mainly optimize textual consistency while insufficiently leveraging visual perception and exploratory dynamics that are essential for multimodal reasoning.

## 3 Methodology

### 3.1 Background and Motivation

GRPO [50] has become a widely used RL algorithm to enhance the reasoning capabilities of large language and vision-language models. It performs policy optimization through group-wise relative evaluation, where multiple responses are sampled for each query and their verifiable rewards are compared to obtain advantages for policy updates. Specifically, for each input query, GRPO generates a group of  $G$  candidate responses and evaluates them using verifiable rewards  $\{R^{(i)}\}_{i=1}^G$  to enable reward-based comparison within the group. From these evaluations, the advantage of the  $i$ -th response is defined as:

$$A^{(i)} = \frac{R^{(i)} - \text{mean}(R^{(j)})}{\text{std}(R^{(j)})}, \quad (1)$$

which represents its relative reward among the sampled responses. During training, this advantage  $A^{(i)}$  is uniformly applied to all tokens of the  $i$ -th response, and the policy parameters are updated using a PPO-style [49] objective:

$$J_G(\theta) = \mathbb{E} \left[ \min(r_t^{(i)} A^{(i)}, \text{clip}(r_t^{(i)}, 1 - \varepsilon, 1 + \varepsilon) A^{(i)}) \right], \quad (2)$$

where  $r_t^{(i)}$  denotes the importance ratio computed from the new and old policies, and  $\varepsilon$  is the clipping threshold that controls the update magnitude for stable policy optimization. From this objective, the policy gradient in GRPO is driven by the sequence-level advantage  $A^{(i)}$ , which is uniformly applied across all tokens within the response.

However, such sequence-level supervision limits optimization granularity, as it ignores the varying semantic and perceptual relevance of individual tokens. This limitation is particularly pronounced in large vision-language models, where visual grounding primarily determines response correctness, whereas textual reasoning contributes

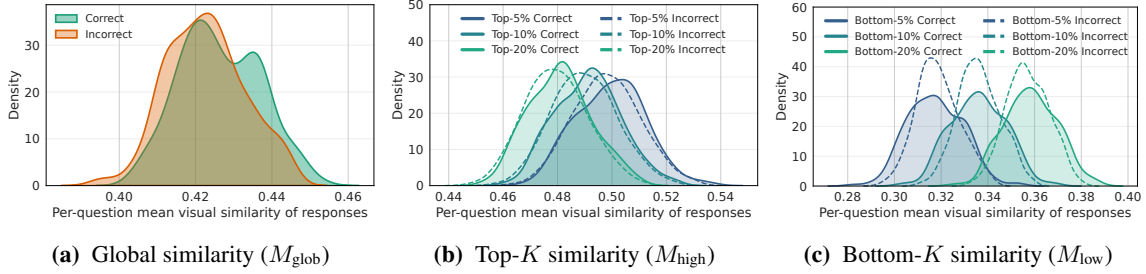


**Figure 2** Distributions of different visual similarity metrics comparing correct and incorrect responses. (a) The global similarity ( $M_{\text{glob}}$ ) across all tokens, where correct responses exhibit a clear rightward shift. (b) The top- $K$  similarity ( $M_{\text{high}}$ ), where the correct-response peak also moves right. (c) The bottom- $K$  similarity ( $M_{\text{low}}$ ), where the shift is negligible. Together, these results show that reasoning correctness is characterized by a subset of visual-grounded tokens.

more extensively to gradient updates, leading to optimization imbalance and weakened perception-reasoning alignment.

### 3.2 Token-Level Analysis of Multimodal Reasoning

To investigate how token-level signals relate to multimodal reasoning behavior, we analyze visual similarity and entropy as complementary indicators of perceptual grounding and reasoning uncertainty. Our analysis is conducted on the Geometry3K dataset [37] using the Qwen2.5-VL-3B-Instruct model [3], sampling 8 responses per question with a decoding temperature of 1.

**Visual similarity analysis.** To quantify the visual dependency of each response token, we define its visual similarity (VS) as the mean cosine similarity between the hidden states of the response token and those of all vision tokens across all model layers:

$$\text{VS}_t = \frac{1}{L} \sum_{l=1}^L \frac{1}{N} \sum_{n=1}^N \frac{\langle h_{l,t}, v_{l,n} \rangle}{\|h_{l,t}\| \|v_{l,n}\|}, \quad (3)$$

where  $L$  denotes the total number of layers,  $N$  the number of vision tokens, and  $h_{l,t}$  and  $v_{l,n}$  represent the hidden states of the  $t$ -th response token and the  $n$ -th vision token at layer  $l$ , respectively.

To assess how visual dependency correlates with response correctness, we aggregate the VS scores within each response across all tokens ( $M_{\text{glob}}$ ), the top- $K$  subset ( $M_{\text{high}}$ ), and the bottom- $K$  subset ( $M_{\text{low}}$ ). For each question, these metrics are computed separately for correct and incorrect responses. As shown in Fig. 2, the distributions of  $M_{\text{glob}}$  and  $M_{\text{high}}$  for correct responses exhibit a clear rightward shift relative to incorrect ones, indicating that successful reasoning places greater weight on a compact subset of visually aligned tokens. In contrast, the  $M_{\text{low}}$  distributions show minimal separation, suggesting that tokens with low visual relevance contribute little to distinguishing response quality. These observations suggest that correctness is associated with increased reliance on visual-grounded tokens.

**Visual-entropy complementarity.** To assess the complementary contributions of visual similarity and entropy, we analyze token partitions defined by these two indicators under controlled perturbations and through their associated semantic patterns. As shown in Fig. 3(a), we conduct a controlled forward pass using identical question-response pairs while removing the image input. Tokens ranked by visual similarity exhibit substantially larger hidden-state shifts under image removal, indicating stronger dependence on visual evidence. In contrast, entropy-ranked tokens show relatively stable representations, suggesting that entropy primarily reflects language uncertainty rather than visual sensitivity. We further analyze the token distributions associated with each partition. Fig. 3(b) shows that high-entropy tokens are enriched with reasoning-transition expressions such as verification, correction, and analysis, which typically mark decision points within the reasoning trajectory. In comparison, Fig. 3(c) illustrates that high visual similarity tokens concentrate on perceptually grounded concepts, including geometric entities and spatial attributes. These observations indicate that visual similarity and entropy encode complementary aspects of multimodal reasoning: the former reflects perceptual grounding, whereas the latter quantifies uncertainty throughout the reasoning process.

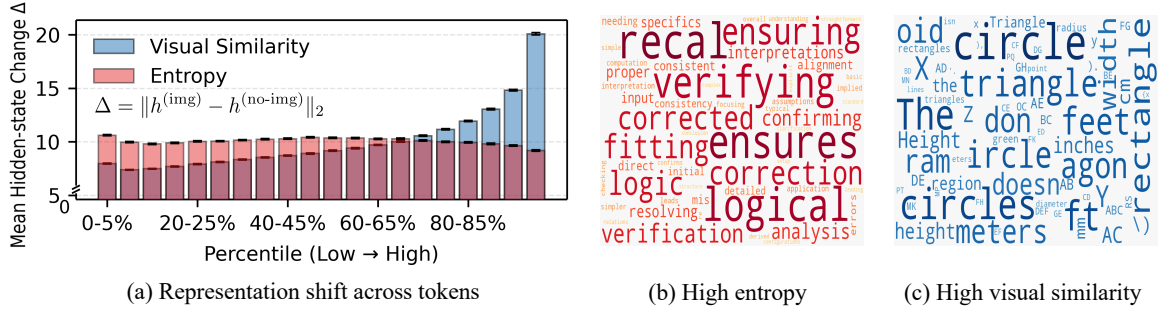


**Figure 3** Token-level analysis of visual similarity and entropy. (a) High visual similarity tokens exhibit larger hidden-state shifts under image removal than high entropy tokens. (b) Word cloud of high entropy tokens and (c) word cloud of high visual similarity tokens, illustrating reasoning-related and perceptual terms.

### 3.3 Perception-Exploration Policy Optimization

Building upon the above analysis, we introduce Perception-Exploration Policy Optimization (PEPO), a token-level reinforcement learning framework that integrates visual perception and exploration to refine reasoning in LVLMs. As illustrated in Fig. 4, PEPO extracts layer-wise hidden states of response and vision tokens from the policy model and computes visual similarity and entropy for each token to capture perceptual grounding and reasoning uncertainty. Our key insight is that visual-grounded tokens anchor perception and high-entropy tokens capture exploratory transitions, which together exhibit complementary roles during multimodal reasoning. To exploit this complementarity, PEPO employs a smooth gating mechanism that fuses visual similarity and entropy to generate adaptive token-level weights. These weights induce token-level advantages that reweight the policy-gradient updates toward visual-grounded and exploratory reasoning tokens, enabling fine-grained optimization that distinguishes the contributions of intermediate reasoning steps.

**Perception modeling.** Based on the analysis in Sec. 3.2 that visual-grounded tokens play a key role in reasoning accuracy, we incorporate a perception prior  $\{VS_t^{(i)}\}_{t=1}^T$  to capture the degree of visual grounding for each token in the  $i$ -th response. To this end, each  $VS_t^{(i)}$  is computed from the hidden-state correlations between response and vision tokens across all transformer layers, serving as a lightweight and supervision-free estimate of perceptual alignment. This design allows tokens with higher  $VS_t^{(i)}$  to receive greater importance during optimization, thereby guiding the model to focus on visual-grounded reasoning steps.

**Exploration modeling.** While the perception modeling captures how strongly each token is grounded in visual content, reasoning dynamics in LVLMs also involve uncertainty and exploratory transitions that perception alone cannot represent. To model this aspect, we introduce an exploration score computed from the token-level entropy sequence  $\{H_t^{(i)}\}_{t=1}^T$  derived from the output logits of the policy model:

$$H_t^{(i)} = - \sum_{x \in \mathcal{V}} p_\theta(x|s_t^{(i)}) \log p_\theta(x|s_t^{(i)}), \quad (4)$$

where  $\mathcal{V}$  denotes the vocabulary and  $p_\theta(x|s_t^{(i)})$  is the model’s predicted probability of token  $x$  at decoding state  $s_t^{(i)}$ . Tokens with higher  $H_t^{(i)}$  correspond to uncertain reasoning steps or transition points, reflecting regions where the model explores multiple reasoning responses. By integrating this exploration signal with perception modeling, PEPO achieves a more fine-grained representation of multimodal reasoning processes.

**Perception-exploration fusion.** To construct a unified optimization framework, we integrate the perception score  $VS_t^{(i)}$  and exploration score  $H_t^{(i)}$  to jointly model perceptual grounding and exploratory uncertainty at the token level. Both scores are min-max normalized to  $[0,1]$  within each response to obtain  $\hat{VS}_t^{(i)}$  and  $\hat{H}_t^{(i)}$ , ensuring comparability and preventing scale bias, and their joint dependency is parameterized through a smooth gating operator:

$$\hat{g}_t^{(i)} = \hat{VS}_t^{(i)} + \hat{H}_t^{(i)} - \text{mean}_t(\hat{VS}^{(i)} + \hat{H}^{(i)}), \quad (5)$$

$$w_t^{(i)} = T \cdot \text{Softmax}((1 + \alpha \tanh(\hat{g}_t^{(i)})) \cdot VS_t^{(i)}), \quad (6)$$

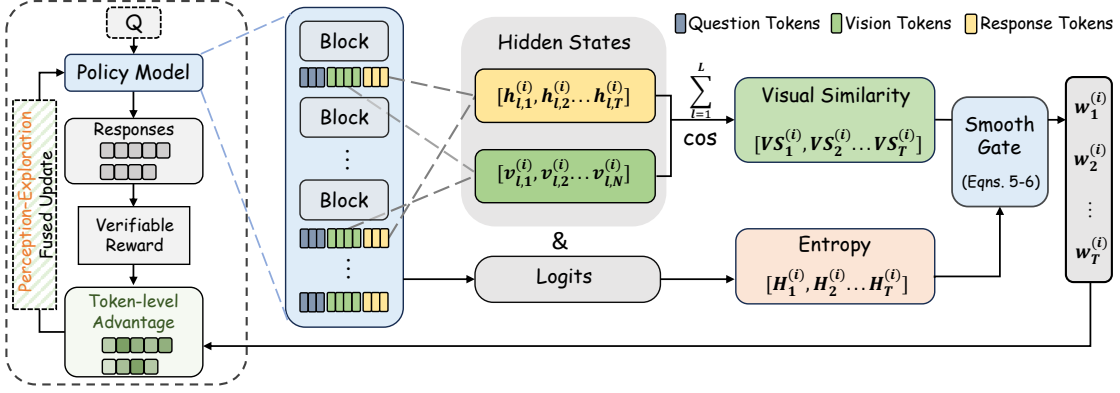


**Figure 4** Framework of PEPO. During response generation, the layer-wise hidden states of response tokens and vision tokens are extracted, along with the output logits. For each response token, visual similarity and entropy are computed, and the centered sum of their normalized values is passed through a smooth gating function to produce token-wise weights that modulate the advantages for PEPO updates.

where  $\hat{g}_t^{(i)}$  denotes the mean-centered joint score derived from the normalized visual similarity and entropy, which is subsequently processed by a  $\tanh(\cdot)$  activation to obtain a smooth gating function. Crucially, the gate is multiplied by  $VS_t^{(i)}$ , which keeps perception dominant and conditions entropy-driven modulation on visually grounded tokens, avoiding indiscriminate amplification of high-entropy but visually irrelevant tokens. Finally,  $T$  rescales the softmax output so that  $\mathbb{E}[w_t^{(i)}] = 1$ , preserving the overall advantage scale while redistributing token-level credit. This operator adaptively assigns token-level weights  $w_t$  by integrating perceptual relevance and reasoning uncertainty, which subsequently guide token-level policy optimization in a fine-grained manner.

**Token-level advantage.** The fused weight  $w_t^{(i)}$  is used to refine the sequence-level advantage computed in GRPO variants. Let  $A^{(i)}$  denote the GRPO advantage for the  $i$ -th response. We define a token-level advantage as:

$$A_t^{(i)} = [(1 - \lambda) + \lambda w_t^{(i)}] A^{(i)}, \quad (7)$$

where  $\lambda$  controls the strength of the token-level modulation, linearly increasing from 0 to 1 over training steps. This formulation yields fine-grained optimization signals that capture the heterogeneous contributions of individual tokens, allowing PEPO to be seamlessly incorporated into policy optimization frameworks while preserving computational efficiency and enhancing perception-reasoning alignment.

## 4 Experiments

### 4.1 Experiment Setup

**Models and baselines.** We conduct experiments using two recent open-source vision-language models, Qwen2.5-VL-3B-Instruct [3] and InternVL3-2B-Instruct [88], both of which exhibit strong multimodal representation and reasoning capabilities. To evaluate effectiveness, PEPO is compared against three representative RL methods: GRPO [50], DAPO [79], and High-Entropy RL [63]. Since PEPO introduces token-level advantage estimation, it remains fully compatible with existing policy optimization frameworks. Two variants are accordingly implemented: PEPO<sub>G</sub>, built upon GRPO, and PEPO<sub>D</sub>, built upon DAPO.

**Datasets.** We evaluate PEPO across five categories of multimodal reasoning tasks. For **geometry reasoning**, training is conducted on Geometry3K [37], and generalization is assessed on MathVista [36], MathVerse [83], and LogicVista [72], reporting average accuracy over 8 responses (avg@8). For **visual grounding**, we use 2K samples from RefCOCO for RL training and evaluate on the validation, testA, and testB splits, with cross-domain evaluation on LISA-Grounding [27] using IoU@50. For **few-shot classification**, we adopt FGVC Aircraft [39] and Flower102 [43] under 1-, 2-, and 4-shot settings to examine data efficiency. For **visual puzzle reasoning**, we randomly sample 1.5K examples from the PuzzleVQA dataset [10] for training and reserve 0.5K for testing, with AlgoPuzzleVQA used for out-of-domain evaluation. Finally, for **scalability analysis**, we train on the large-scale

**Table 1** Results on Geometry3K validation/test splits and out-of-domain benchmarks, including MathVista, MathVerse, and LogicVista.

Method	Geometry3K <sub>val</sub>	Geometry3K <sub>test</sub>	MathVista <sub>mini</sub>	MathVerse <sub>mini</sub>	LogicVista	Avg
<i>Qwen2.5-VL-3B-Instruct</i>						
Base (zero-shot)	11.58	14.25	50.19	37.66	32.22	29.18
High-Entropy RL	15.58	18.26	50.69	39.84	32.59	31.39
GRPO	19.00	23.79	51.56	40.54	28.30	32.64
PEPO <sub>G</sub> (Ours)	21.91	27.27	54.45	45.42	34.45	36.70 (+4.06)
DAPO	22.63	27.00	53.68	44.44	33.13	36.18
PEPO <sub>D</sub> (Ours)	22.38	27.89	54.75	44.23	33.89	36.63 (+0.45)
<i>InternVL3-2B-Instruct</i>						
Base (zero-shot)	7.88	9.03	23.00	23.36	28.36	18.33
High-Entropy RL	10.89	8.30	35.24	20.70	17.18	18.46
GRPO	22.08	26.33	49.36	42.09	28.84	33.74
PEPO <sub>G</sub> (Ours)	25.84	31.28	52.36	44.89	31.88	37.25 (+3.51)
DAPO	20.94	21.57	50.40	41.11	28.52	32.51
PEPO <sub>D</sub> (Ours)	28.12	31.18	51.49	45.24	32.25	37.66 (+5.15)

**Table 2** IoU@50 on RefCOCO and out-of-domain LISA with Qwen2.5-VL-3B-Instruct. The High-Entropy RL collapses in 3 runs, so its results are omitted.

Method	RefCOCO			LISA	Avg
	val	testA	testB		
Base (zero-shot)	89.10	91.70	84.00	56.51	80.33
High-Entropy RL	model collapsed (no valid results)				
GRPO	90.12	92.29	85.55	62.42	82.60
PEPO <sub>G</sub> (Ours)	90.44	92.40	85.75	65.26	83.46 (+0.86)
DAPO	90.10	92.40	85.08	62.48	82.52
PEPO <sub>D</sub> (Ours)	90.03	92.72	85.42	64.23	83.10 (+0.58)

**Table 3** Few-shot (1/2/4-shot) results on the FGVC Aircraft and Flower102 datasets. All methods are trained and evaluated using the Qwen2.5-VL-3B-Instruct backbone.

Dataset	Method	1-shot	2-shot	4-shot	Avg
FGVC	SFT	36.24	40.86	55.48	44.19
	GRPO	48.72	55.60	63.94	56.09
	PEPO <sub>G</sub>	51.13	57.31	75.79	61.41 (+5.32)
Flower102	SFT	33.98	44.50	52.33	43.60
	GRPO	53.23	57.94	66.22	59.13
	PEPO <sub>G</sub>	54.81	59.44	67.52	60.59 (+1.46)

ViRL39K dataset [61] and evaluate on diverse reasoning benchmarks including Geometry3K<sub>test</sub>, MathVista, We-Math [45], MathVerse, LogicVista, SuperClevr Counting [30], and MMMU-Pro [82].

**Implementation details.** All models are trained under a unified RLVR framework using the default verifiable rewards defined by each dataset. The hyperparameter  $\alpha$  is tuned separately for each dataset due to task differences. We use AdamW [35] as the optimizer with full-parameter fine-tuning, bfloat16 precision, and gradient checkpointing enabled to reduce memory consumption. For each question, we sample 8 responses using a temperature of 1.0 and top- $p = 1.0$ , and train with DeepSpeed ZeRO-2 [47] for efficient distributed optimization. All RLVR methods are implemented within the Swift framework [86] and all experiments are conducted on 8 NVIDIA A40 GPUs. Additional implementation details are provided in the supplementary material.

## 4.2 Main Results

**Overall performance.** Across all benchmarks and model architectures, PEPO consistently outperforms GRPO, DAPO, and High-Entropy RL in both reasoning accuracy and training stability. Compared with GRPO, High-Entropy RL shows unstable optimization and weaker multimodal reasoning performance, as it relies solely on entropy-driven exploration without perceptual grounding. These results show that visual grounding complements entropy-based exploration in achieving robust multimodal reasoning. By integrating visual similarity to strengthen perception and token entropy to guide exploration, PEPO achieves stable optimization and notable performance gains across tasks. We next present detailed evaluations on geometry reasoning, visual grounding, and few-shot classification, followed by results on visual puzzle reasoning.

**Geometry reasoning.** Tab. 1 presents results on Geometry3K and three out-of-domain benchmarks, MathVista, MathVerse, and LogicVista. On Qwen2.5-VL-3B, PEPO improves the average score over GRPO by +3.67

**Table 4** Accuracy (%) on PuzzleVQA and out-of-domain AlgoPuzzleVQA datasets.

Method	Qwen2.5-VL-3B-Instruct			InternVL3-2B-Instruct		
	PuzzleVQA	AlgoPuzzleVQA	Avg	PuzzleVQA	AlgoPuzzleVQA	Avg
Base (zero-shot)	31.80	21.72	26.76	31.80	23.00	27.40
High-Entropy RL	35.00	24.61	29.81	32.60	25.22	28.91
GRPO	43.20	25.44	34.32	43.20	26.17	34.69
PEPO <sub>G</sub> (Ours)	45.00	26.94	35.97 (+1.65)	45.20	27.22	36.21 (+1.52)
DAPO	44.60	25.33	34.97	44.80	27.72	36.26
PEPO <sub>D</sub> (Ours)	46.80	26.56	36.68 (+1.71)	45.20	28.61	36.91 (+0.65)

**Table 5** Comparison of scaling performance among GRPO, PAPO, and PEPO on Qwen2.5-VL-3B-Instruct trained with ViRL39K, evaluated across multiple reasoning benchmarks using the avg@8 metric. GRPO and PAPO results are taken directly from [67].

Method	Geometry3K <sub>test</sub>	MathVista	We-Math	MathVerse	LogicVista	Counting	MMMU-Pro	Avg
GRPO	28.72	59.34	58.90	55.25	38.14	55.81	25.66	45.97
PAPO <sub>G</sub>	30.95	61.38	60.09	57.14	38.67	62.56	27.11	48.27
PEPO <sub>G</sub> (Ours)	29.85	63.48	60.98	56.49	39.85	70.75	27.47	49.84 (+3.87)

points and over DAPO by +0.45 points. On InternVL3-2B, the improvements over GRPO and DAPO are +3.51 and +5.15 points. Larger performance gains on MathVerse and LogicVista indicate that PEPO is effective on benchmarks requiring integrated visual and symbolic reasoning.

**Visual grounding.** Tab. 2 presents results on RefCOCO and the out-of-domain LISA-Grounding dataset evaluated by IoU@50. On RefCOCO, PEPO achieves comparable or slightly higher accuracy than GRPO and DAPO across all validation and test splits, indicating stable in-domain performance. More evident improvements are observed on LISA-Grounding, where PEPO shows clear gains in localization accuracy under domain shift. These results suggest that weighting tokens by visual similarity improves the alignment between textual and visual representations.

**Few-shot classification.** Following [34], we evaluate the training effectiveness of PEPO under limited data settings. As shown in Tab. 3, PEPO consistently outperforms GRPO across the 1-shot, 2-shot, and 4-shot settings, markedly enhancing few-shot classification performance on both FGVC Aircraft and Flower102 datasets. Compared to GRPO, PEPO<sub>G</sub> achieves average gains of +5.32 and +1.46 points on the two datasets, respectively. These results demonstrate that our fine-grained advantage modulation enhances training effectiveness by enabling the policy model to better leverage limited supervision for improved generalization.

**Visual puzzle reasoning.** Similar to the geometry reasoning results, Tab. 4 presents that PEPO achieves consistent improvements on both in-domain and out-of-domain puzzle reasoning benchmarks. Across the two backbones, PEPO obtains higher accuracy than GRPO and DAPO on both PuzzleVQA and AlgoPuzzleVQA. The relative gain is also evident on the out-of-domain AlgoPuzzleVQA dataset, where reasoning requires recognizing abstract relational and compositional patterns beyond surface visual cues. These results indicate that the proposed visual similarity weighting enhances visuospatial reasoning and facilitates transfer to unseen puzzle configurations.

**Scalability analysis.** To examine how PEPO scales with larger datasets and more complex reasoning scenarios, we train the Qwen2.5-VL-3B-Instruct model on the ViRL39K dataset and evaluate it on several reasoning benchmarks. We follow the training configurations of PAPO [67] in terms of learning rate and KL penalty coefficient, and adopt the same prompt and reward design to ensure a fair comparison. As shown in Tab. 5, PEPO<sub>G</sub> achieves higher average performance than GRPO and PAPO<sub>G</sub>, demonstrating superior scalability with larger datasets and more complex reasoning tasks. The gains are particularly evident on perception-intensive datasets such as MathVista and Counting, where visual grounding is crucial for reasoning.

**Efficiency and computational overhead.** We evaluate the training efficiency of PEPO in Tab. 6 by reporting end-to-end throughput (iterations per second), mean response length, and the step-level computational overhead ratio  $\rho$ . The overhead ratio is defined as  $\rho = t_{\text{weight}}/t_{\text{step}}$ , where  $t_{\text{weight}}$  denotes the time required to compute  $VS_t$ ,  $H_t$ , and  $w_t$ , and  $t_{\text{step}}$  is the total time of a reinforcement learning update step. Across all benchmarks,  $\rho$  remains below 1%, indicating that the additional computation introduced by PEPO is negligible relative to the overall training cost. Throughput is comparable to, and in some cases slightly higher than, that of GRPO. We

**Table 6** Training efficiency comparison between GRPO and PEPO<sub>G</sub>. We report throughput (iterations per second), mean response length, and the step-level computational overhead ratio  $\rho$  across datasets. The overhead ratio  $\rho$  measures the proportion of additional weight computation time within a full RL update step.

Metric	Method	Geometry3K	PuzzleVQA	RefCOCO	FGVC Aircraft
Iter/s	GRPO	0.022	0.066	0.080	0.071
	PEPO <sub>G</sub>	0.022	0.074	0.084	0.083
Mean length	GRPO	273	104	77	92
	PEPO <sub>G</sub>	270	85	64	77
$\rho$	PEPO <sub>G</sub>	0.0039	0.0065	0.0061	0.0048

**Table 7** Ablation of PEPO components. Perception-only uses visual similarity for weighting ( $\alpha = 0$ ), while Exploration-only relies on token entropy.

Variant	Geometry3K <sub>val</sub>	PuzzleVQA
GRPO (baseline)	19.00	43.20
Exploration-only	20.18	41.60
Perception-only	21.07	43.20
PEPO <sub>G</sub>	22.80	45.00

**Table 8** Sensitivity to the weight  $\alpha$ . Results are reported on FGVC (4-shot), PuzzleVQA, and geometry reasoning.

$\alpha$	Geometry (Avg)	FGVC (4-shot)
GRPO	32.64	63.94
0.00	36.17	75.48
0.02	36.01	75.79
0.05	36.70	72.97
0.10	36.31	68.17
0.15	36.02	70.39

also observe that PEPO tends to produce shorter responses during training. This reduction in average generation length partially compensates for the minor overhead of weight computation, resulting in similar or improved effective throughput.

### 4.3 Ablation Study

We conduct ablation experiments on the Qwen2.5-VL-3B-Instruct model to examine the effectiveness of PEPO. The analysis includes the effect of visual and entropy components and the influence of different weighting schemes.

**Component analysis.** Tab. 7 analyzes the effect of individual components in PEPO on Geometry3K, PuzzleVQA, and RefCOCO. Using only visual similarity (perception-only) enhances perceptual grounding but limits reasoning diversity, while relying solely on entropy (exploration-only) introduces unstable optimization and reduced accuracy. The full visual-entropy formulation integrates both factors and achieves the best results, indicating their complementary roles in stabilizing learning and encouraging diverse yet coherent reasoning. These results show that balanced perception-exploration coupling is essential for token-level policy optimization in multimodal reasoning.

**Sensitivity and robustness of  $\alpha$ .** Tab. 8 analyzes the impact of the weighting coefficient  $\alpha$  on both perception-intensive (FGVC Aircraft) and reasoning-oriented (Geometry reasoning) benchmarks. All non-zero  $\alpha$  settings consistently outperform the GRPO baseline across tasks. For Geometry reasoning, introducing a small positive  $\alpha$  leads to clear improvements, and performance remains stable across a moderate range of values, indicating limited sensitivity to precise tuning. For FGVC Aircraft, smaller  $\alpha$  values yield the strongest gains, while larger values gradually reduce the improvement, although performance remains above the baseline throughout.

**Weighting design.** Tab. 9 evaluates the effect of different weighting formulations on Geometry3K. Removing the gradual scheduling strategy leads to a substantial performance drop, indicating that progressive modulation of token weights is important for stable optimization. Excluding per-sample min-max normalization also degrades performance, suggesting that normalization helps maintain consistent scaling across tokens within each response. Replacing the gated formulation with a simple additive fusion further reduces accuracy. This result indicates that the bounded and mean-centered gating mechanism provides a more stable integration of perceptual and entropy signals than direct summation.

**Layer selection.** Tab. 10 analyzes the impact of restricting the hidden-state layers used for weight computation. Using features from shallow, intermediate, or deep layers alone consistently underperforms the default configuration. In contrast, aggregating signals across all layers yields the highest accuracy, suggesting that visual

**Table 9** Removing scheduling, normalization, or gating degrades performance.

Variant	Geometry3K <sub>val</sub>	Geometry3K <sub>Test</sub>
PEPO <sub>G</sub>	22.80	26.81
W/o schedule	19.80	24.54
W/o min-max	21.91	26.93
Additive fusion	20.99	22.94

**Table 10** Effect of restricting the hidden-state layers used for weight computation in PEPO.

Layer range	Geometry3K <sub>val</sub>	Geometry3K <sub>Test</sub>
1–10	18.92	23.71
11–20	22.04	25.75
21–32	19.89	24.94

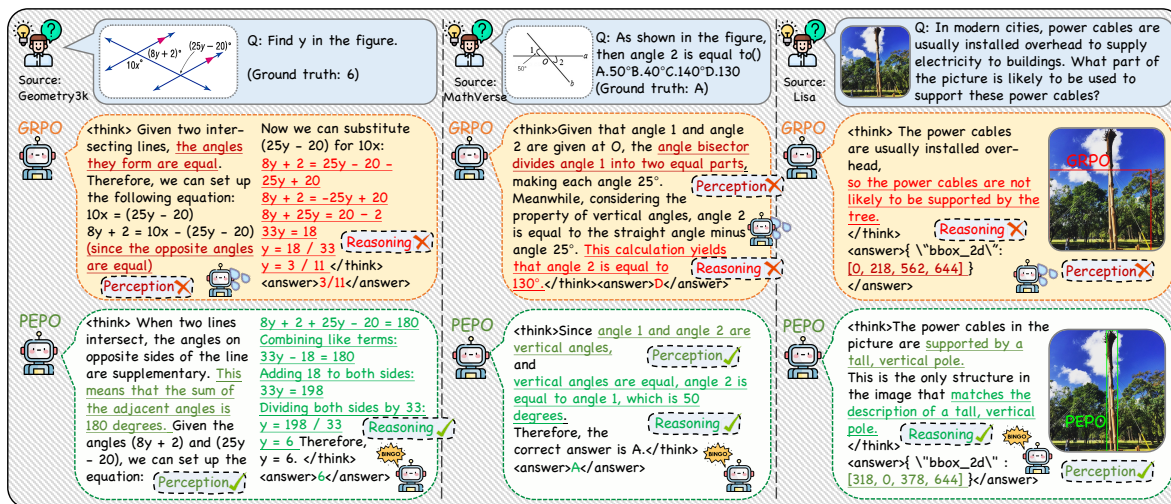


**Figure 5** Qualitative comparison on Geometry3K, MathVerse, and LISA datasets. The GRPO-trained model exhibits perception failures and inconsistent reasoning, leading to incorrect answers. In contrast, the PEPO-trained model generates coherent, visually grounded reasoning chains that produce correct results, demonstrating the effectiveness of PEPO in enhancing multimodal reasoning.

relevance is distributed across the model hierarchy rather than localized to a specific depth.

#### 4.4 Qualitative Comparisons

**Case studies.** Fig. 5 presents representative examples from geometry reasoning (Geometry3K), mathematical derivation (MathVerse), and visual grounding (LISA). In the geometry example, GRPO incorrectly manipulates angle relations despite the diagram indicating supplementary structure, revealing a failure to align algebraic operations with visual constraints. In the mathematical derivation case, GRPO introduces inconsistent intermediate conclusions, leading to a contradiction in the final answer. For visual grounding, GRPO misidentifies salient regions in the image, reflecting insufficient reliance on perceptual evidence. In contrast, PEPO maintains alignment between visual cues and intermediate reasoning steps. It correctly extracts geometric relations from the diagram, preserves logical consistency in algebraic transformations, and grounds its predictions on visually relevant structures in the image. Across tasks, the reasoning trajectories generated by PEPO remain coherent and consistent with the available visual evidence, resulting in correct final predictions.

**Training dynamics.** Fig. 6 compares the optimization behavior of GRPO and PEPO<sub>G</sub> on FGVC Aircraft (4-shot). PEPO<sub>G</sub> attains consistently higher training reward and converges to a stronger plateau. The mean response length under PEPO<sub>G</sub> decreases more gradually during training, resulting in shorter generations. In addition, PEPO<sub>G</sub> exhibits a progressively increasing mean visual similarity, whereas GRPO shows a weaker or declining trend. Regarding entropy, GRPO undergoes a sharper decay, while PEPO<sub>G</sub> maintains a more moderate entropy level throughout training. These results indicate that PEPO<sub>G</sub> yields more stable optimization dynamics across reward, generation length, visual alignment, and exploration behavior.

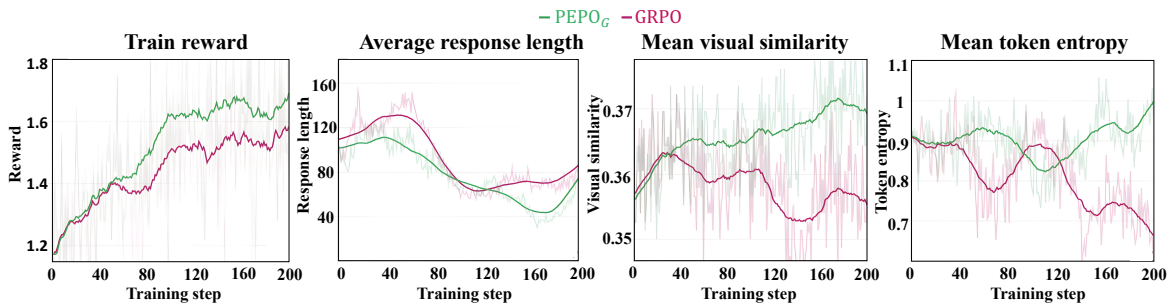


**Figure 6** Training curves on FGVC Aircraft (4-shot). We compare GRPO and PEPO<sub>G</sub> in terms of training reward, mean response length, mean visual similarity, and mean entropy.

## 5 Conclusions

We present Perception-Exploration Policy Optimization (PEPO), a token-level reinforcement learning framework for large vision-language models. By coupling visual similarity and token entropy through a smooth gating mechanism, PEPO achieves fine-grained advantage estimation that jointly models perceptual grounding and reasoning exploration. Based on two different architectures, extensive experiments demonstrate that PEPO consistently outperforms GRPO and DAPO across geometry reasoning, visual puzzles, visual grounding, and few-shot classification, while maintaining training stability and scalability on large multimodal datasets. These results confirm that integrating perception and exploration offers a principled and effective approach to advancing multimodal reasoning in LVLMs.

## References

- [1] Inclusion AI, Fudong Wang, Jiajia Liu, Jingdong Chen, Jun Zhou, Kaixiang Ji, Lixiang Ru, Qingpei Guo, Ruobing Zheng, Tianqi Li, et al. M2-reasoning: Empowering mllms with unified general and spatial reasoning. *arXiv preprint arXiv:2507.08306*, 2025. 3
- [2] Stanislaw Antol, Aishwarya Agrawal, Jiasen Lu, Margaret Mitchell, Dhruv Batra, C Lawrence Zitnick, and Devi Parikh. Vqa: Visual question answering. In *Proceedings of the IEEE international conference on computer vision*, pages 2425–2433, 2015. 1
- [3] Shuai Bai, Keqin Chen, Xuejing Liu, Jialin Wang, Wenbin Ge, Sibao Song, Kai Dang, Peng Wang, Shijie Wang, Jun Tang, et al. Qwen2. 5-vl technical report. *arXiv preprint arXiv:2502.13923*, 2025. 1, 2, 4, 6
- [4] Sule Bai, Mingxing Li, Yong Liu, Jing Tang, Haoji Zhang, Lei Sun, Xiangxiang Chu, and Yansong Tang. Univ-r1: Reasoning guided universal visual grounding with reinforcement learning. *arXiv preprint arXiv:2505.14231*, 2025. 3
- [5] Keqin Chen, Zhao Zhang, Weili Zeng, Richong Zhang, Feng Zhu, and Rui Zhao. Shikra: Unleashing multimodal llm’s referential dialogue magic. *arXiv preprint arXiv:2306.15195*, 2023. 3
- [6] Liang Chen, Hongcheng Gao, Tianyu Liu, Zhiqi Huang, Flood Sung, Xinyu Zhou, Yuxin Wu, and Baobao Chang. G1: Bootstrapping perception and reasoning abilities of vision-language model via reinforcement learning. *arXiv preprint arXiv:2505.13426*, 2025. 3
- [7] Liang Chen, Lei Li, Haozhe Zhao, and Yifan Song. Vinci. r1-v: Reinforcing super generalization ability in vision-language models with less than 3, 2025. 1
- [8] Minghan Chen, Guikun Chen, Wenguan Wang, and Yi Yang. Seed-grpo: Semantic entropy enhanced grpo for uncertainty-aware policy optimization. *arXiv preprint arXiv:2505.12346*, 2025. 1, 3
- [9] Yi Chen, Yuying Ge, Rui Wang, Yixiao Ge, Junhao Cheng, Ying Shan, and Xihui Liu. Grpo-care: Consistency-aware reinforcement learning for multimodal reasoning. *arXiv preprint arXiv:2506.16141*, 2025. 3

- [10] Yew Ken Chia, Vernon Toh Yan Han, Deepanway Ghosal, Lidong Bing, and Soujanya Poria. Diagnosing multimodal reasoning challenges of language models with abstract visual patterns. *arXiv preprint arXiv:2403.13315*, 2024. 2, 6
- [11] Ganqu Cui, Yuchen Zhang, Jiacheng Chen, Lifan Yuan, Zhi Wang, Yuxin Zuo, Haozhan Li, Yuchen Fan, Huayu Chen, Weize Chen, et al. The entropy mechanism of reinforcement learning for reasoning language models. *arXiv preprint arXiv:2505.22617*, 2025. 3
- [12] Tri Dao. Flashattention-2: Faster attention with better parallelism and work partitioning. *arXiv preprint arXiv:2307.08691*, 2023. 18
- [13] Tri Dao, Dan Fu, Stefano Ermon, Atri Rudra, and Christopher R’e. Flashattention: Fast and memory-efficient exact attention with io-awareness. *Advances in neural information processing systems*, 35:16344–16359, 2022. 1
- [14] Yihe Deng, Hritik Bansal, Fan Yin, Nanyun Peng, Wei Wang, and Kai-Wei Chang. Openvlthinker: An early exploration to complex vision-language reasoning via iterative self-improvement. *arXiv preprint arXiv:2503.17352*, 2025. 3
- [15] Kaixuan Fan, Kaituo Feng, Haoming Lyu, Dongzhan Zhou, and Xiangyu Yue. Sophiavl-r1: Reinforcing mllms reasoning with thinking reward. *arXiv preprint arXiv:2505.17018*, 2025. 3
- [16] Yue Fan, Xuehai He, Diji Yang, Kaizhi Zheng, Ching-Chen Kuo, Yuting Zheng, Sravana Jyothi Narayanaraju, Xinze Guan, and Xin Eric Wang. Grit: Teaching mllms to think with images. *arXiv preprint arXiv:2505.15879*, 2025. 3
- [17] Yunhao Gou, Kai Chen, Zhili Liu, Lanqing Hong, Xin Jin, Zhenguo Li, James T Kwok, and Yu Zhang. Perceptual decoupling for scalable multi-modal reasoning via reward-optimized captioning. *arXiv preprint arXiv:2506.04559*, 2025. 3
- [18] Yash Goyal, Tejas Khot, Douglas Summers-Stay, Dhruv Batra, and Devi Parikh. Making the v in vqa matter: Elevating the role of image understanding in visual question answering. In *Proceedings of the IEEE conference on computer vision and pattern recognition*, pages 6904–6913, 2017. 1
- [19] Daya Guo, Dejian Yang, Haowei Zhang, Junxiao Song, Peiyi Wang, Qihao Zhu, Runxin Xu, Ruoyu Zhang, Shirong Ma, Xiao Bi, et al. Deepseek-r1 incentivizes reasoning in llms through reinforcement learning. *Nature*, 645(8081):633–638, 2025. 1, 2, 3
- [20] Siyuan Huang, Xiaoye Qu, Yafu Li, Yun Luo, Zefeng He, Daizong Liu, and Yu Cheng. Spotlight on token perception for multimodal reinforcement learning. *arXiv preprint arXiv:2510.09285*, 2025. 1
- [21] Aaron Hurst, Adam Lerer, Adam P Goucher, Adam Perelman, Aditya Ramesh, Aidan Clark, AJ Ostrow, Akila Welihinda, Alan Hayes, Alec Radford, et al. Gpt-4o system card. *arXiv preprint arXiv:2410.21276*, 2024. 1
- [22] Pu Jian, Junhong Wu, Wei Sun, Chen Wang, Shuo Ren, and Jiajun Zhang. Look again, think slowly: Enhancing visual reflection in vision-language models. In *Proceedings of the 2025 Conference on Empirical Methods in Natural Language Processing*, pages 9262–9281, 2025. 1
- [23] Chaoya Jiang, Yongrui Heng, Wei Ye, Han Yang, Haiyang Xu, Ming Yan, Ji Zhang, Fei Huang, and Shikun Zhang. Vlm-r 3: Region recognition, reasoning, and refinement for enhanced multimodal chain-of-thought. *arXiv preprint arXiv:2505.16192*, 2025. 3
- [24] Qing Jiang, Xingyu Chen, Zhaoyang Zeng, Junzhi Yu, and Lei Zhang. Rex-thinker: Grounded object referring via chain-of-thought reasoning. *arXiv preprint arXiv:2506.04034*, 2025. 3
- [25] Sahar Kazemzadeh, Vicente Ordonez, Mark Matten, and Tamara Berg. Referitgame: Referring to objects in photographs of natural scenes. In *Proceedings of the 2014 conference on empirical methods in natural language processing (EMNLP)*, pages 787–798, 2014. 1
- [26] Woosuk Kwon, Zhuohan Li, Siyuan Zhuang, Ying Sheng, Lianmin Zheng, Cody Hao Yu, Joseph E. Gonzalez, Hao Zhang, and Ion Stoica. Efficient memory management for large language model serving with pagedattention. In *Proceedings of the ACM SIGOPS 29th Symposium on Operating Systems Principles*, 2023. 18

- [27] Xin Lai, Zhuotao Tian, Yukang Chen, Yanwei Li, Yuhui Yuan, Shu Liu, and Jiaya Jia. Lisa: Reasoning segmentation via large language model. In *Proceedings of the IEEE/CVF Conference on Computer Vision and Pattern Recognition*, pages 9579–9589, 2024. 1, 2, 6
- [28] Lin Li, Wei Chen, Jiahui Li, Kwang-Ting Cheng, and Long Chen. Relation-rl: Progressively cognitive chain-of-thought guided reinforcement learning for unified relation comprehension. *arXiv preprint arXiv:2504.14642*, 2025. 3
- [29] Ming Li, Jike Zhong, Shitian Zhao, Yuxiang Lai, Haoquan Zhang, Wang Bill Zhu, and Kaipeng Zhang. Think or not think: A study of explicit thinking in rule-based visual reinforcement fine-tuning. *arXiv preprint arXiv:2503.16188*, 2025. 3
- [30] Zhuowan Li, Xingrui Wang, Elias Stengel-Eskin, Adam Kortylewski, Wufei Ma, Benjamin Van Durme, and Alan L Yuille. Super-clevr: A virtual benchmark to diagnose domain robustness in visual reasoning. In *Proceedings of the IEEE/CVF conference on computer vision and pattern recognition*, pages 14963–14973, 2023. 7
- [31] Yiqing Liang, Jieli Qiu, Wenhao Ding, Zuxin Liu, James Tompkin, Mengdi Xu, Mengzhou Xia, Zhengzhong Tu, Laixi Shi, and Jiacheng Zhu. Modomodo: Multi-domain data mixtures for multimodal llm reinforcement learning. *arXiv preprint arXiv:2505.24871*, 2025. 3
- [32] Xiangyan Liu, Jinjie Ni, Zijian Wu, Chao Du, Longxu Dou, Haonan Wang, Tianyu Pang, and Michael Qizhe Shieh. Noisyrollout: Reinforcing visual reasoning with data augmentation. *arXiv preprint arXiv:2504.13055*, 2025. 1
- [33] Yuqi Liu, Tianyuan Qu, Zhisheng Zhong, Bohao Peng, Shu Liu, Bei Yu, and Jiaya Jia. Visionreasoner: Unified visual perception and reasoning via reinforcement learning. *arXiv preprint arXiv:2505.12081*, 2025. 1, 3
- [34] Ziyu Liu, Zeyi Sun, Yuhang Zang, Xiaoyi Dong, Yuhang Cao, Haodong Duan, Dahua Lin, and Jiaqi Wang. Visual-rft: Visual reinforcement fine-tuning. *arXiv preprint arXiv:2503.01785*, 2025. 3, 8
- [35] Ilya Loshchilov and Frank Hutter. Decoupled weight decay regularization. *arXiv preprint arXiv:1711.05101*, 2017. 7, 17
- [36] Pan Lu, Hritik Bansal, Tony Xia, Jiacheng Liu, Chunyuan Li, Hannaneh Hajishirzi, Hao Cheng, Kai-Wei Chang, Michel Galley, and Jianfeng Gao. Mathvista: Evaluating mathematical reasoning of foundation models in visual contexts. *arXiv preprint arXiv:2310.02255*, 2023. 1, 2, 6
- [37] Pan Lu, Ran Gong, Shibiao Jiang, Liang Qiu, Siyuan Huang, Xiaodan Liang, and Song-Chun Zhu. Inter-gps: Interpretable geometry problem solving with formal language and symbolic reasoning. *arXiv preprint arXiv:2105.04165*, 2021. 2, 4, 6
- [38] Yan Ma, Linge Du, Xuyang Shen, Shaoxiang Chen, Pengfei Li, Qibing Ren, Lizhuang Ma, Yuchao Dai, Pengfei Liu, and Junjie Yan. One rl to see them all: Visual triple unified reinforcement learning. *arXiv preprint arXiv:2505.18129*, 2025. 1, 3
- [39] Subhransu Maji, Esa Rahtu, Juho Kannala, Matthew Blaschko, and Andrea Vedaldi. Fine-grained visual classification of aircraft. *arXiv preprint arXiv:1306.5151*, 2013. 2, 6
- [40] Fanqing Meng, Lingxiao Du, Zongkai Liu, Zhixiang Zhou, Quanfeng Lu, Daocheng Fu, Tiancheng Han, Botian Shi, Wenhai Wang, Junjun He, et al. Mm-eureka: Exploring the frontiers of multimodal reasoning with rule-based reinforcement learning. *arXiv preprint arXiv:2503.07365*, 2025. 3
- [41] Chancharik Mitra, Brandon Huang, Trevor Darrell, and Roei Herzig. Compositional chain-of-thought prompting for large multimodal models. In *Proceedings of the IEEE/CVF Conference on Computer Vision and Pattern Recognition*, pages 14420–14431, 2024. 3
- [42] Minheng Ni, Zhengyuan Yang, Linjie Li, Chung-Ching Lin, Kevin Lin, Wangmeng Zuo, and Lijuan Wang. Point-rft: Improving multimodal reasoning with visually grounded reinforcement finetuning. *arXiv preprint arXiv:2505.19702*, 2025. 3
- [43] Maria-Elena Nilsback and Andrew Zisserman. Automated flower classification over a large number of classes. In *2008 Sixth Indian conference on computer vision, graphics image processing*, pages 722–729. IEEE, 2008. 2, 6

- [44] Zhiliang Peng, Wenhui Wang, Li Dong, Yaru Hao, Shaohan Huang, Shuming Ma, and Furu Wei. Kosmos-2: Grounding multimodal large language models to the world. *arXiv preprint arXiv:2306.14824*, 2023. 3
- [45] Runqi Qiao, Qiuna Tan, Guanting Dong, Minhui Wu, Chong Sun, Xiaoshuai Song, Zhuoma GongQue, Shanglin Lei, Zhe Wei, Miaoxuan Zhang, et al. We-math: Does your large multimodal model achieve human-like mathematical reasoning? *arXiv preprint arXiv:2407.01284*, 2024. 1, 7
- [46] Runqi Qiao, Qiuna Tan, Peiqing Yang, Yanzi Wang, Xiaowan Wang, Enhui Wan, Sitong Zhou, Guanting Dong, Yuchen Zeng, Yida Xu, et al. We-math 2.0: A versatile mathbook system for incentivizing visual mathematical reasoning. *arXiv preprint arXiv:2508.10433*, 2025. 1, 3
- [47] Jeff Rasley, Samyam Rajbhandari, Olatunji Ruwase, and Yuxiong He. Deepspeed: System optimizations enable training deep learning models with over 100 billion parameters. In *Proceedings of the 26th ACM SIGKDD international conference on knowledge discovery & data mining*, pages 3505–3506, 2020. 7, 17
- [48] Gabriel Sarch, Snigdha Saha, Naitik Khandelwal, Ayush Jain, Michael J Tarr, Aviral Kumar, and Katerina Fragkiadaki. Grounded reinforcement learning for visual reasoning. *arXiv preprint arXiv:2505.23678*, 2025. 3
- [49] John Schulman, Filip Wolski, Prafulla Dhariwal, Alec Radford, and Oleg Klimov. Proximal policy optimization algorithms. *arXiv preprint arXiv:1707.06347*, 2017. 3
- [50] Zhihong Shao, Peiyi Wang, Qihao Zhu, Runxin Xu, Junxiao Song, Xiao Bi, Haowei Zhang, Mingchuan Zhang, YK Li, Yang Wu, et al. Deepseekmath: Pushing the limits of mathematical reasoning in open language models. *arXiv preprint arXiv:2402.03300*, 2024. 1, 2, 3, 6
- [51] Chuming Shen, Wei Wei, Xiaoye Qu, and Yu Cheng. Satori-r1: Incentivizing multimodal reasoning with spatial grounding and verifiable rewards. *arXiv preprint arXiv:2505.19094*, 2025. 1, 3
- [52] Haozhan Shen, Peng Liu, Jingcheng Li, Chunxin Fang, Yibo Ma, Jiajia Liao, Qiaoli Shen, Zilun Zhang, Kangjia Zhao, Qianqian Zhang, et al. Vlm-r1: A stable and generalizable r1-style large vision-language model. *arXiv preprint arXiv:2504.07615*, 2025. 3
- [53] Alex Su, Haozhe Wang, Weiming Ren, Fangzhen Lin, and Wenhui Chen. Pixel reasoner: Incentivizing pixel-space reasoning with curiosity-driven reinforcement learning. *arXiv preprint arXiv:2505.15966*, 2025. 3
- [54] Zhaochen Su, Linjie Li, Mingyang Song, Yunzhuo Hao, Zhengyuan Yang, Jun Zhang, Guanjie Chen, Jiawei Gu, Juntao Li, Xiaoye Qu, et al. Openthinking: Learning to think with images via visual tool reinforcement learning. *arXiv preprint arXiv:2505.08617*, 2025. 3
- [55] Dídac Surís, Sachit Menon, and Carl Vondrick. Vipergpt: Visual inference via python execution for reasoning. In *Proceedings of the IEEE/CVF international conference on computer vision*, pages 11888–11898, 2023. 3
- [56] Richard S Sutton, David McAllester, Satinder Singh, and Yishay Mansour. Policy gradient methods for reinforcement learning with function approximation. *Advances in neural information processing systems*, 12, 1999. 19
- [57] Huajie Tan, Yuheng Ji, Xiaoshuai Hao, Minglan Lin, Pengwei Wang, Zhongyuan Wang, and Shanghang Zhang. Reason-rft: Reinforcement fine-tuning for visual reasoning. *arXiv preprint arXiv:2503.20752*, 2025. 3
- [58] Gemini Team, Petko Georgiev, Ving Ian Lei, Ryan Burnell, Libin Bai, Anmol Gulati, Garrett Tanzer, Damien Vincent, Zhufeng Pan, Shibo Wang, et al. Gemini 1.5: Unlocking multimodal understanding across millions of tokens of context. *arXiv preprint arXiv:2403.05530*, 2024. 1
- [59] Abdullah Vanlioglu. Entropy-guided sequence weighting for efficient exploration in rl-based llm fine-tuning. *arXiv preprint arXiv:2503.22456*, 2025. 3
- [60] Zhongwei Wan, Zhihao Dou, Che Liu, Yu Zhang, Dongfei Cui, Qinjian Zhao, Hui Shen, Jing Xiong, Yi Xin, Yifan Jiang, et al. Srpo: Enhancing multimodal llm reasoning via reflection-aware reinforcement learning. *arXiv preprint arXiv:2506.01713*, 2025. 3

- [61] Haozhe Wang, Chao Qu, Zuming Huang, Wei Chu, Fangzhen Lin, and Wenhui Chen. VI-rethinker: Incentivizing self-reflection of vision-language models with reinforcement learning. *arXiv preprint arXiv:2504.08837*, 2025. 2, 3, 7
- [62] Jiawei Wang, Jiakai Liu, Yuqian Fu, Yingru Li, Xintao Wang, Yuan Lin, Yu Yue, Lin Zhang, Yang Wang, and Ke Wang. Harnessing uncertainty: Entropy-modulated policy gradients for long-horizon llm agents. *arXiv preprint arXiv:2509.09265*, 2025. 1, 3
- [63] Shenzhi Wang, Le Yu, Chang Gao, Chujie Zheng, Shixuan Liu, Rui Lu, Kai Dang, Xionghui Chen, Jianxin Yang, Zhenru Zhang, et al. Beyond the 80/20 rule: High-entropy minority tokens drive effective reinforcement learning for llm reasoning. *arXiv preprint arXiv:2506.01939*, 2025. 1, 3, 6
- [64] Weiyun Wang, Zhangwei Gao, Lixin Gu, Hengjun Pu, Long Cui, Xingguang Wei, Zhaoyang Liu, Linglin Jing, Shenglong Ye, Jie Shao, et al. Internvl3. 5: Advancing open-source multimodal models in versatility, reasoning, and efficiency. *arXiv preprint arXiv:2508.18265*, 2025. 1, 3
- [65] Xiyao Wang, Zhengyuan Yang, Chao Feng, Yongyuan Liang, Yuhang Zhou, Xiaoyu Liu, Ziyi Zang, Ming Li, Chung-Ching Lin, Kevin Lin, et al. Vicrit: A verifiable reinforcement learning proxy task for visual perception in vlms. *arXiv preprint arXiv:2506.10128*, 2025. 3
- [66] Xiyao Wang, Zhengyuan Yang, Chao Feng, Hongjin Lu, Linjie Li, Chung-Ching Lin, Kevin Lin, Furong Huang, and Lijuan Wang. Sota with less: Mcts-guided sample selection for data-efficient visual reasoning self-improvement. *arXiv preprint arXiv:2504.07934*, 2025. 1
- [67] Zhenhailong Wang, Xuehang Guo, Sofia Stoica, Haiyang Xu, Hongru Wang, Hyeonjeong Ha, Xiuxi Chen, Yangyi Chen, Ming Yan, Fei Huang, et al. Perception-aware policy optimization for multimodal reasoning. *arXiv preprint arXiv:2507.06448*, 2025. 1, 8
- [68] Jason Wei, Xuezhi Wang, Dale Schuurmans, Maarten Bosma, Fei Xia, Ed Chi, Quoc V Le, Denny Zhou, et al. Chain-of-thought prompting elicits reasoning in large language models. *Advances in neural information processing systems*, 35:24824–24837, 2022. 1
- [69] Junfei Wu, Jian Guan, Kaituo Feng, Qiang Liu, Shu Wu, Liang Wang, Wei Wu, and Tieniu Tan. Reinforcing spatial reasoning in vision-language models with interwoven thinking and visual drawing. *arXiv preprint arXiv:2506.09965*, 2025. 3
- [70] Tianhe Wu, Jian Zou, Jie Liang, Lei Zhang, and Kede Ma. Visualquality-r1: Reasoning-induced image quality assessment via reinforcement learning to rank. *arXiv preprint arXiv:2505.14460*, 2025. 3
- [71] Tong Xiao, Xin Xu, Zhenya Huang, Hongyu Gao, Quan Liu, Qi Liu, and Enhong Chen. Advancing multimodal reasoning capabilities of multimodal large language models via visual perception reward. *arXiv preprint arXiv:2506.07218*, 2025. 1, 3
- [72] Yijia Xiao, Edward Sun, Tianyu Liu, and Wei Wang. Logicvista: Multimodal llm logical reasoning benchmark in visual contexts. *arXiv preprint arXiv:2407.04973*, 2024. 2, 6
- [73] Guowei Xu, Peng Jin, Ziang Wu, Hao Li, Yibing Song, Lichao Sun, and Li Yuan. Llava-cot: Let vision language models reason step-by-step. In *Proceedings of the IEEE/CVF International Conference on Computer Vision*, pages 2087–2098, 2025. 3
- [74] Yi Xu, Chengzu Li, Han Zhou, Xingchen Wan, Caiqi Zhang, Anna Korhonen, and Ivan Vulic. Visual planning: Let’s think only with images. *arXiv preprint arXiv:2505.11409*, 2025. 3
- [75] Biao Yang, Bin Wen, Boyang Ding, Changyi Liu, Chenglong Chu, Chengru Song, Chongling Rao, Chuan Yi, Da Li, Dunju Zang, et al. Kwai keye-vl 1.5 technical report. *arXiv preprint arXiv:2509.01563*, 2025. 1
- [76] Yi Yang, Xiaoxuan He, Hongkun Pan, Xiyan Jiang, Yan Deng, Xingtao Yang, Haoyu Lu, Dacheng Yin, Fengyun Rao, Minfeng Zhu, et al. R1-onevision: Advancing generalized multimodal reasoning through cross-modal formalization. *arXiv preprint arXiv:2503.10615*, 2025. 3
- [77] En Yu, Kangheng Lin, Liang Zhao, Jisheng Yin, Yana Wei, Yuang Peng, Haoran Wei, Jianjian Sun, Chunrui Han, Zheng Ge, et al. Perception-r1: Pioneering perception policy with reinforcement learning. *arXiv preprint arXiv:2504.07954*, 2025. 3

- [78] Licheng Yu, Patrick Poirson, Shan Yang, Alexander C Berg, and Tamara L Berg. Modeling context in referring expressions. In *European conference on computer vision*, pages 69–85. Springer, 2016. 1, 2
- [79] Qiyang Yu, Zheng Zhang, Ruofei Zhu, Yufeng Yuan, Xiaochen Zuo, Yu Yue, Weinan Dai, Tiantian Fan, Gaohong Liu, Lingjun Liu, et al. Dapo: An open-source llm reinforcement learning system at scale. *arXiv preprint arXiv:2503.14476*, 2025. 2, 3, 6
- [80] Wenwen Yu, Zhibo Yang, Yuliang Liu, and Xiang Bai. Dothinker: Explainable multimodal large language models with rule-based reinforcement learning for document understanding. In *Proceedings of the IEEE/CVF International Conference on Computer Vision*, pages 837–847, 2025. 1
- [81] Ruifeng Yuan, Chenghao Xiao, Sicong Leng, Jianyu Wang, Long Li, Weiwen Xu, Hou Pong Chan, Deli Zhao, Tingyang Xu, Zhongyu Wei, et al. V1-cogito: Progressive curriculum reinforcement learning for advanced multimodal reasoning. *arXiv preprint arXiv:2507.22607*, 2025. 3
- [82] Xiang Yue, Tianyu Zheng, Yuansheng Ni, Yubo Wang, Kai Zhang, Shengbang Tong, Yuxuan Sun, Botao Yu, Ge Zhang, Huan Sun, et al. Mmmu-pro: A more robust multi-discipline multimodal understanding benchmark. In *Proceedings of the 63rd Annual Meeting of the Association for Computational Linguistics (Volume 1: Long Papers)*, pages 15134–15186, 2025. 7
- [83] Renrui Zhang, Dongzhi Jiang, Yichi Zhang, Haokun Lin, Ziyu Guo, Pengshuo Qiu, Aojun Zhou, Pan Lu, Kai-Wei Chang, Yu Qiao, et al. Mathverse: Does your multi-modal llm truly see the diagrams in visual math problems? In *European Conference on Computer Vision*, pages 169–186. Springer, 2024. 1, 2, 6
- [84] Ruohong Zhang, Bowen Zhang, Yanghao Li, Haotian Zhang, Zhiqing Sun, Zhe Gan, Yinfei Yang, Ruoming Pang, and Yiming Yang. Improve vision language model chain-of-thought reasoning. In *Proceedings of the 63rd Annual Meeting of the Association for Computational Linguistics (Volume 1: Long Papers)*, pages 1631–1662, 2025. 3
- [85] Xintong Zhang, Zhi Gao, Bofei Zhang, Pengxiang Li, Xiaowen Zhang, Yang Liu, Tao Yuan, Yuwei Wu, Yunde Jia, Song-Chun Zhu, et al. Chain-of-focus: Adaptive visual search and zooming for multimodal reasoning via rl. *arXiv preprint arXiv:2505.15436*, 2025. 3
- [86] Yuze Zhao, Jintao Huang, Jinghan Hu, Xingjun Wang, Yunlin Mao, Daoze Zhang, Zeyinzi Jiang, Zhikai Wu, Baole Ai, Ang Wang, et al. Swift: a scalable lightweight infrastructure for fine-tuning. In *AAAI*, volume 39, pages 29733–29735, 2025. 7, 17
- [87] Ziwei Zheng, Michael Yang, Jack Hong, Chenxiao Zhao, Guohai Xu, Le Yang, Chao Shen, and Xing Yu. Deepeyes: Incentivizing” thinking with images” via reinforcement learning. *arXiv preprint arXiv:2505.14362*, 2025. 3
- [88] Jinguo Zhu, Weiyun Wang, Zhe Chen, Zhaoyang Liu, Shenglong Ye, Lixin Gu, Hao Tian, Yuchen Duan, Weijie Su, Jie Shao, et al. Internvl3: Exploring advanced training and test-time recipes for open-source multimodal models. *arXiv preprint arXiv:2504.10479*, 2025. 1, 2, 6
- [89] Linghao Zhu, Yiran Guan, Dingkan Liang, Jianzhong Ju, Zhenbo Luo, Bin Qin, Jian Luan, Yuliang Liu, and Xiang Bai. Shuffle-r1: Efficient rl framework for multimodal large language models via data-centric dynamic shuffle. *arXiv preprint arXiv:2508.05612*, 2025. 1
- [90] Muzhi Zhu, Hao Zhong, Canyu Zhao, Zongze Du, Zheng Huang, Mingyu Liu, Hao Chen, Cheng Zou, Jingdong Chen, Ming Yang, et al. Active-o3: Empowering multimodal large language models with active perception via grpo. *arXiv preprint arXiv:2505.21457*, 2025. 3

# Appendix

## A Implementation Details

This section provides additional implementation details for our experiments. For clarity, we organize the experiments into five task settings that share the same RLVR training framework but differ in data sources and hyperparameter configurations:

- Task 1: Geometry and logic reasoning. Experiments on Geometry3K, MathVista, MathVerse, and LogicVista.
- Task 2: Visual grounding. Experiments on RefCOCO and LISA-Grounding.
- Task 3: Few-shot classification. Experiments on FGVC Aircraft and Flower102 under 1/2/4-shot settings.
- Task 4: Visual puzzle reasoning. Experiments on PuzzleVQA and AlgoPuzzleVQA.
- Task 5: Scalability analysis. Experiments on ViRL39K and the multi-benchmark evaluation used for the scaling experiments in the main paper.

Across all settings, we adopt a unified RLVR setup. As summarized in Tab. 1, we use AdamW [35] with full-parameter fine-tuning in bfloat16 precision and gradient checkpointing. For each question, we sample 8 responses with temperature 1.0 and top- $p = 1.0$ , and train with DeepSpeed ZeRO-2 [47] on 8 NVIDIA A40 GPUs. All RLVR methods are implemented within the Swift framework [86]. The gate strength  $\alpha$  is constrained to a small shared set across tasks:  $\alpha = 0.1$  for Tasks 1/4/5,  $\alpha = 0.05$  for Task 2, and  $\alpha = 0.02$  for Task 3.

## B Prompt and Reward Design

The design of prompts and verifiable rewards plays a central role in RLVR, as it governs both how the model articulates its reasoning and how reliable responses can be evaluated. Tab. 2 summarizes the prompt formats and rewards used across the five task settings. All tasks employ simple, programmatically verifiable reward components to ensure deterministic and reproducible evaluation. The format reward verifies whether a response adheres strictly to the prescribed output template (e.g., correct use of `<think>` / `<answer>` tags, JSON format for visual grounding, and the `\boxed{\}` wrapper in Task 5), and assigns a value of 1 only when all format checks are satisfied. The accuracy reward is binary: the final prediction is extracted from the `<answer>` span (Tasks 1, 3, 4) or from the content within `\boxed{\}` (Task 5), and correctness is determined using ground-truth annotations or the official evaluation script. For visual grounding (Task 2), the IoU reward is given directly as the intersection-over-union value between the predicted box and the best-matching ground-truth box. The overall rewards for each sample are the weighted sum of these components, as specified in Tab. 2. To ensure unambiguous evaluation, all prompts instruct the model to output its intermediate reasoning within `<think> ... </think>` before producing a concise answer in a designated format (either `<answer> ... </answer>` or `\boxed{\}`), which is used exclusively for reward computation.

## C Evaluation

We adopt the standard dataset splits and employ deterministic, programmatic evaluation.

**Geometry and logic reasoning.** For Geometry3K (validation and test), MathVista-mini, MathVerse-mini, and LogicVista, we report accuracy averaged over multiple samples. For each image-question pair, the model generates 8 responses with temperature set to 1.0, and computes the avg@8 accuracy. To avoid any LLM-as-a-judge evaluation and ensure that correctness is decided purely by programmatic rules, we omit instances with free-form answers on all geometry reasoning out-of-domain datasets, except MathVista-mini, which is evaluated strictly using the official script released by the authors, including their normalization and correctness checker.

**Few-shot classification.** For FGVC Aircraft and Flower102, we follow the 1-, 2-, and 4-shot settings described in the experiment setup section of the main paper (Sec. 4.1). The support images and labels are included in the prompt, and the model predicts the class name of the query image via greedy decoding. A prediction is considered correct if the decoded class name exactly matches the ground-truth category label.

**Table 1** Key hyperparameters across the five tasks.

Hyperparameter	Task(s)	Value
<i>Shared RL configuration</i>		
Optimizer	1–5	AdamW
Train type	1–5	full
Precision	1–5	bfloat16
Gradient checkpointing	1–5	Enabled
Responses per question	1–5	8
Temperature	1–5	1.0
Top-p	1–5	1.0
DeepSpeed stage	1–5	ZeRO-2
Iterations	1–5	1
Freeze Vision Tower	1–5	True
<i>Optimization hyperparameters</i>		
Learning rate	1, 4, 5	$1 \times 10^{-6}$
Learning rate	2, 3	$2 \times 10^{-6}$
LR schedule	1–4	Cosine
LR schedule	5	Constant
Per-device train batch size	1, 3	2
Per-device train batch size	2, 4, 5	4
Gradient accumulation steps	1	4
Gradient accumulation steps	2, 3, 4	2
Gradient accumulation steps	5	32
Epochs	1, 2, 4	1
Epochs	3	4
Epochs	5	2
KL coefficient $\beta$	1–4	0.001
KL coefficient $\beta$	5	0.01
<i>Context length and generation</i>		
Use vLLM [26]	1–5	True
Attention implementation	1–5	FlashAttention2 [12]
Max completion length	1, 5	1024
Max completion length	2, 3, 4	512
<i>DAPO specific hyperparameters</i>		
Clip Ratio Low	1–5	0.2
Clip Ratio High	1–5	0.28
Loss Averaging Mode	1–5	Token-level
Max Resample Times	1–5	3
<i>High-entropy RL specific hyperparameters</i>		
Top Entropy Quantile	1–5	0.2
<i>PEPO specific hyperparameters</i>		
Gate alpha	4, 5	0.1
Gate alpha	1, 2	0.05
Gate alpha	3	0.02

**Table 2** Prompt and reward design across the five tasks.

Task(s)	Design
<i>Reward Design</i>	
1, 3, 4	Format reward + Accuracy reward
2	Format reward + IoU reward
5	$0.1 \times$ Format reward + $0.9 \times$ Accuracy reward
<i>Prompt Design</i>	
1	First output the thinking process in <code>&lt;think&gt; ... &lt;/think&gt;</code> tags and then output the final answer in <code>&lt;answer&gt; ... &lt;/answer&gt;</code> tags.
2	First output the thinking process in <code>&lt;think&gt; ... &lt;/think&gt;</code> tags and then output the final answer in <code>&lt;answer&gt; ... &lt;/answer&gt;</code> tags. Output the final answer in JSON format.
3	This is an image containing an aircraft/plant. Please identify the model of the aircraft/plant based on the image. Output the thinking process in <code>&lt;think&gt; ... &lt;/think&gt;</code> and the final answer in <code>&lt;answer&gt; ... &lt;/answer&gt;</code> tags. The output format should be: <code>&lt;think&gt; ... &lt;/think&gt; &lt;answer&gt;species name&lt;/answer&gt;</code> . Please strictly follow the format.
4	First output the thinking process in <code>&lt;think&gt; ... &lt;/think&gt;</code> tags and then output the final answer in <code>&lt;answer&gt; ... &lt;/answer&gt;</code> tags. Answer with the option letter directly.
5	First think through the reasoning process as an internal monologue, enclosed within <code>&lt;think&gt; ... &lt;/think&gt;</code> tags. Then provide the final answer enclosed within <code>\boxed{\}</code> .

**Visual puzzle reasoning.** For PuzzleVQA and AlgoPuzzleVQA, we report top-1 accuracy. Each question is associated with a predefined set of options, and the model outputs a single option label enclosed in `<answer> ... </answer>` tags. We use greedy decoding, and any malformed or ambiguous output is treated as incorrect.

**Visual grounding.** For RefCOCO and LISA-Grounding, we follow the standard phrase grounding protocol and report IoU@50. The model predicts a single bounding box using greedy decoding (temperature 0). A prediction is deemed correct if the predicted bounding box attains an IoU of at least 0.5 with any ground-truth annotation.

**Scaling benchmarks.** For the ViRL39K scalability experiments, models are trained on ViRL39K and evaluated on Geometry3K<sub>test</sub>, MathVista, We-Math, MathVerse, LogicVista, SuperClevr Counting, and MMMU-Pro. We employ the public evaluation scripts from PAPO to ensure fair comparison. Following PAPO, instances requiring an LLM-as-a-judge are excluded for all datasets except Geometry3K, ensuring that all reported metrics rely solely on deterministic checkers. All benchmarks adopt the same avg@8 protocol described above.

## D Policy Gradient View of PEPO

In Alg. 1, PEPO introduces token-wise weights  $\{w_t^{(i)}\}_{t=1}^T$  to refine the sequence-level advantage of GRPO. We show that the unit-mean constraint on  $w_t^{(i)}$  preserves the sequence-level policy-gradient scale and only redistributes credit among tokens.

**Unit-mean property.** For a response of length  $T$  we set

$$w_t^{(i)} = T \cdot \text{Softmax}(z_t^{(i)}), \quad (1)$$

so that

$$\frac{1}{T} \sum_{t=1}^T w_t^{(i)} = \sum_{t=1}^T \text{Softmax}(z_t^{(i)}) = 1 \implies \sum_{t=1}^T w_t^{(i)} = T. \quad (2)$$

**Effect on the policy gradient.** For response  $i$ , the (unclipped) GRPO policy gradient [56] can be written as

$$\nabla_{\theta} J_G(\theta) = \mathbb{E} \left[ \sum_{t=1}^T A^{(i)} \nabla_{\theta} \log \pi_{\theta}(x | s_t^{(i)}) \right], \quad (3)$$

where  $A^{(i)}$  is the sequence-level advantage. In PEPO, we use token-wise advantages

$$A_t^{(i)} = [(1 - \lambda) + \lambda w_t^{(i)}] A^{(i)}. \quad (4)$$

---

**Algorithm 1** Perception–Exploration Policy Optimization (PEPO)

---

**Require:** Policy  $\pi_\theta$ , old policy  $\pi_{\text{old}}$ , group size  $G$ , maximum steps  $K_{\text{max}}$ , gate strength  $\alpha$ , learning rate  $\eta$

- 1: **for**  $k = 1, \dots, K_{\text{max}}$  **do**
  - 2:   Sample prompts and grouped responses  $\{\tau^{(i)}\}_{i=1}^G$  from  $\pi_{\text{old}}$
  - 3:   Compute rewards  $R^{(i)}$  and GRPO advantages
  - 4:    $A^{(i)} \leftarrow \frac{R^{(i)} - \text{mean}_j R^{(j)}}{\text{std}_j R^{(j)} + \varepsilon}$
  - 5:   **Perception modeling (visual similarity):**
  - 6:   For each token  $t$  in response  $i$ , compute
  - 7:    $\text{VS}_t^{(i)} \leftarrow \frac{1}{L} \sum_{l=1}^L \frac{1}{N} \sum_{n=1}^N \frac{\langle h_{l,t}^{(i)}, v_{l,n}^{(i)} \rangle}{\|h_{l,t}^{(i)}\| \|v_{l,n}^{(i)}\|}$
  - 8:   **Exploration modeling (entropy):**
  - 9:   For each token  $t$  in response  $i$ , compute
  - 10:    $H_t^{(i)} \leftarrow - \sum_{x \in \mathcal{V}} p_\theta(x | s_t^{(i)}) \log p_\theta(x | s_t^{(i)})$
  - 11:   **Perception–exploration fusion:**
  - 12:   Min–max normalize  $\text{VS}_t^{(i)}$  and  $H_t^{(i)}$  over  $t$  to obtain  $\hat{\text{VS}}_t^{(i)}, \hat{H}_t^{(i)} \in [0, 1]$
  - 13:    $\hat{g}_t^{(i)} \leftarrow \hat{\text{VS}}_t^{(i)} + \hat{H}_t^{(i)} - \text{mean}_t(\hat{\text{VS}}^{(i)} + \hat{H}^{(i)})$
  - 14:    $w_t^{(i)} \leftarrow T \cdot \text{Softmax}_t((1 + \alpha \tanh(\hat{g}_t^{(i)})) \text{VS}_t^{(i)})$
  - 15:   **Token-level advantage:**
  - 16:    $\lambda_k \leftarrow \min(1, k/K_{\text{max}})$
  - 17:    $A_t^{(i)} \leftarrow [(1 - \lambda_k) + \lambda_k w_t^{(i)}] A^{(i)}$
  - 18:   **Policy update:**
  - 19:   Use  $A_t^{(i)}$  in place of  $A^{(i)}$  in a standard GRPO / PPO-style objective  $J(\theta)$
  - 20:    $\theta \leftarrow \theta + \eta \nabla_\theta J(\theta)$
  - 21:    $\pi_{\text{old}} \leftarrow \pi_\theta$
  - 22: **end for**
- 

The total advantage per sequence becomes

$$\begin{aligned} \sum_{t=1}^T A_t^{(i)} &= A^{(i)} \sum_{t=1}^T [(1 - \lambda) + \lambda w_t^{(i)}] \\ &= A^{(i)} [(1 - \lambda)T + \lambda \sum_{t=1}^T w_t^{(i)}] \\ &= A^{(i)} T, \end{aligned} \tag{5}$$

Therefore, PEPO preserves the total sequence-level advantage mass  $TA^{(i)}$  and does not introduce a global scaling change in the policy gradient. The modification affects only the distribution of credit across tokens within the summation in Eqn. 3. As a result, the overall gradient magnitude remains consistent with GRPO, while credit is preferentially allocated to visually grounded or high-entropy tokens.

## E Additional Ablation Results

The main paper examines the roles of perception and exploration in PEPO and the key elements of its weighting strategy. Here we provide additional ablations to further characterize the method under different settings.

**Effect of gate strength  $\alpha$ .** To investigate how entropy interacts with visual similarity, we vary the gate strength  $\alpha$  in the perception–exploration fusion module. As shown in Tab. 3, PEPO remains robust across a range of  $\alpha$  values. The perception-only variant ( $\alpha = 0$ ) already outperforms GRPO, indicating that visual similarity alone provides a strong training signal. Adding a moderate entropy gate further improves performance, with the best average results obtained at  $\alpha = 0.05$  or  $\alpha = 0.10$  depending on the benchmark. When  $\alpha$  is chosen

**Table 3** Ablation on gate strength  $\alpha$  of PEPO on geometry and logic reasoning benchmarks using the Qwen2.5-VL-3B-Instruct model.

$\alpha$	Geometry3K <sub>val</sub>	Geometry3K <sub>test</sub>	MathVista <sub>mini</sub>	MathVerse <sub>mini</sub>	LogicVista	Avg
0.00 (Perception-only)	21.07	26.73	52.81	45.31	34.93	36.17
0.02	20.60	25.87	53.88	44.99	34.73	36.01
0.05 (Default)	21.91	27.27	54.45	45.42	34.45	36.70
0.10	22.80	26.81	53.58	44.12	34.26	36.31
0.15	21.45	26.52	53.54	43.99	34.62	36.02

**Table 4** Ablation on perception prior measures used to compute visual similarity.

Measure	Geometry3K <sub>val</sub>	Geometry3K <sub>test</sub>	FGVC Aircraft (4-shot)
L1 distance	19.00	24.50	60.85
L2 distance	20.90	26.08	67.33
Cosine similarity (Default)	22.80	26.81	75.79

either too small or too large, the overall performance drops slightly. This trend suggests that entropy is most beneficial when it serves as a complementary modulation signal rather than being completely removed or overly amplified. Overall, the results support both the robustness of PEPO to  $\alpha$  and the effectiveness of using a modest gate strength.

**Effect of perception prior measure.** We analyze the impact of different similarity measures used to compute the perception prior in PEPO. Our default choice is the cosine similarity between hidden states and visual embeddings, motivated by its scale invariance and its widespread effectiveness in vision–language alignment (e.g., CLIP-style representations). We compare cosine similarity with two distance-based alternatives, namely L1 and L2 distances. As shown in Tab. 4, cosine similarity consistently achieves better performance across geometry reasoning and few-shot classification benchmarks. In particular, replacing cosine similarity with L1 or L2 distance leads to noticeable performance degradation, indicating that cosine similarity provides a more stable and semantically aligned signal for perception modeling.

## F Additional Details for the Hidden-state Shift Analysis

**Hidden-state shift across tokens.** The bar plot in the main paper summarizes the hidden-state shift of response tokens when grouped into bins defined by their visual similarity or token-level entropy. Given hidden states  $h_{l,t}^{\text{with}}$  and  $h_{l,t}^{\text{without}}$  for token  $t$  at layer  $l$  with and without the image input, respectively, the representational shift associated with token  $t$  is defined as

$$D_t = \frac{1}{L} \sum_{l=1}^L \|h_{l,t}^{\text{with}} - h_{l,t}^{\text{without}}\|_2. \tag{6}$$

Tokens are then assigned to percentile bins according to either their visual similarity  $VS_t$  or their entropy, both computed under the image-present condition, and we report the average value of  $D_t$  within each bin.

**Word cloud construction.** The word clouds in this analysis illustrate lexical patterns associated with high-entropy and high-visual-similarity tokens. To construct these word clouds, we aggregate per-token statistics over Geometry3K as follows:

- Tokens with fewer than 50 occurrences are excluded to avoid instability due to rare or noisy items.
- For entropy-based clouds, tokens are ranked by their mean token-level entropy; for perception-based clouds, they are ranked by their mean visual similarity  $VS_t$ .
- From each ranking, we select a fixed set of the top 100 tokens and weight them by their aggregated frequencies when rendering the clouds.
- Special tokens and non-semantic artifacts (e.g., control tokens and markup) are removed.

## **G Limitations**

Although we demonstrate the effectiveness of PEPO on recent 2B or 3B LVLMs under several RLVR training pipelines, we do not extend our experiments to larger model backbones (e.g., 7B or above) or to longer-context configurations due to computational and memory limitations. Furthermore, our evaluation is confined to a curated set of multimodal reasoning and grounding benchmarks. Applying PEPO to stronger base models and to a broader range of tasks, such as video understanding and tool-augmented reasoning, is an important direction for future research.